Hindawi Publishing Corporation
International Journal of Photoenergy
Volume 2012, Article ID 987606, 8 pages
doi:10.1155/2012/987606

Research Article

Photosensitized Oxidation of 9,10-Dimethylanthracene on Dye-Doped Silica Composites

Elim Albiter, Salvador Alfaro, and Miguel A. Valenzuela

Laboratorio Catálisis y Materiales, ESIQIE Instituto Politécnico Nacional, Zacatenco, 07738 México City, DF, Mexico

Correspondence should be addressed to Miguel A. Valenzuela, mavalenz@ipn.mx

Received 15 July 2011; Accepted 17 November 2011

Academic Editor: Shifu Chen

A series of cationic dyes, methylene blue (MB), safranin O (SF), toluidine blue (TB), and neutral red (NR), were successfully incorporated into a silica matrix by using ultrasound irradiation during the Stöber process. Several analyses were performed, including scanning dynamic light scattering (DLS), electron microscopy (SEM), nitrogen physisorption, FTIR spectroscopy, UV-vis, and diffuse reflectance spectroscopy. The entrapped dyes on silica were evaluated in singlet oxygen ($^1O_2$) generation under visible light irradiation, by means of the photosensitized oxidation of 9,10-dimethylanthracene (DMA). According to the results, the photocatalytic performance of the silica composites was improved, and the leakage of the dye from the particles was suppressed. Among these four different types of dye-doped silica composites, the SiO_2-SF composite showed the most efficient delivery of $^1O_2$.

1. Introduction

A photosensitized reaction is defined as the process leading to photochemical or photophysical changes in a substrate by means of the absorption of radiation by other entity called a photosensitizer [1]. Since the 1960s, several fundamental works have been published related to photosensitization in presence of oxygen and have distinguished two competing mechanisms referred as Type I and Type II [2–5]. Type I photooxygenation involves the formation of a sensitizer triplet state ($^3S^*$) which interacts with a substrate (XH) giving rise to a pair of free radicals by electron-transfer or hydrogen-transfer mechanisms [1]. These produced radicals react with oxygen to regenerate the sensitizer and to form peroxy or superoxide radicals. Type II mechanism implicates the direct interaction of the sensitizer excited state with oxygen, generating upon energy transfer singlet oxygen [$^1O_2$, ($^1\Delta_g$)] which reacts directly with numerous organic substrates [6].

In spite of many efforts and successful results in the study of photosensitized reactions in homogeneous media, there are some disadvantages by this route mainly due to the solubility of the sensitizers in the reaction solvent and their removal from the reaction mixture [7]. These problems can be overcome by the immobilization of the sensitizer in appropriated solid carriers. For instance, the advantages of using a dye dispersed on a solid carrier are the oligomerization of the dye can be prevented, a higher photostability of the dye is obtained, a higher purity of the final products, and the reusability of the dye [8]. Important applications, for example, fine chemical synthesis, wastewater treatment, and photodynamic processes, among others, have been found for photosensitized singlet oxygen production [7–14].

Although many solid carriers such as polymers, zeolites, semiconductors, glasses, silica gel, among others, have been used to support a variety of sensitizers [15], we are interested to develop a hybrid organic-inorganic systems made of dye-doped silica particles active under visible-light irradiation for fine chemical synthesis. Silica is a very attractive material for many industrial and medical applications because it is inexpensive, chemically inert, thermally stable, and biocompatible. In fact, silica particles have captured much attention over the past two decades for their application in catalysis, separation, biosensors, and adsorption [16]. Silica particles can be tuned from 50 to 300 nm containing pore diameters between 2 and 10 nm allowing for different dyes loadings. Also, they have a high surface area (>700 m^2/g) and large pore volume (>0.9 mL/g) allowing high loading of chemicals [16]. The doping of organic dyes into a silica matrix is not an easy task due to the weak interaction between the organic-inorganic hybrid compound [17]. Usually, the main

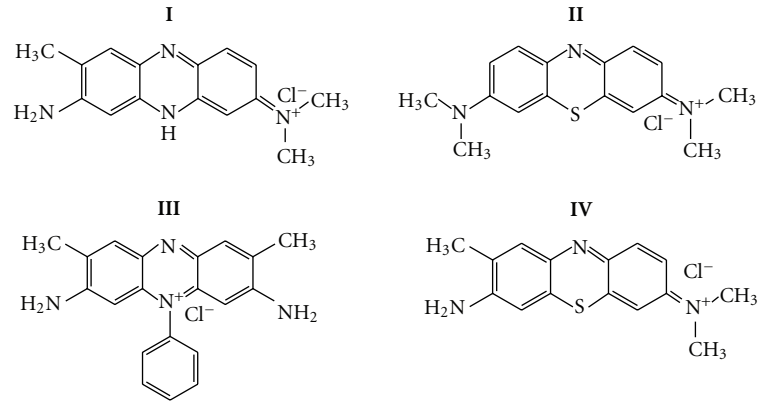

Figure 1: Molecular structure of the dyes: (**I**) neutral red (NR), (**II**) methylene blue (MB), (**III**) safranin O (SF), and (**IV**) toluidine blue O (TB).

problem to solve is the instability of the composites, and dye molecules with small size are easy to leak out from the matrix [17]. Several approaches have been developed to incorporate organic dyes into a silica matrix, for instance, covalent coupling [18], reverse microemulsion [19], and electrostatic interaction (Stöber method) [20]. However, there is still no effective method to control the dispersion of the dye molecules, since they are quickly and spontaneously accumulated into the silica particles [21].

Herein, we reported a simple and modified Stöber method to synthesize SiO_2-dyes composites by employing ultrasound irradiation during the hydrolysis and condensation steps of the silica source and dye addition. It was found that the as-synthesized composites were well dispersed into the silica particles with high stability during the photooxidation of 9,10-dimethylanthracene under visible light.

2. Experimental

2.1. Synthesis of SiO_2-Dye Composites. Tetraethyl orthosilicate (TEOS), methylene blue (MB), safranin O (SF), toluidine blue (TB), neutral red (NR), and SiO_2 nanopowder were purchased from Sigma-Aldrich and used without further purification. Ethanol (HPLC grade) was used as solvent; double distilled water and ammonium hydroxide (NH_4OH) were also used during the synthesis. The molecular structure of the dyes can be seen in Figure 1.

The composites were synthesized by using a modified Stöber method where the dye was incorporated since the formation of the SiO_2 particles. TEOS was used as silica source and NH_4OH as catalyst, and the composites silica-dye were obtained in one-step process. Briefly, it was prepared two solutions, one containing TEOS and ethanol (solution 1) and another with NH_4OH, water, and dye (solution 2). Solution 1 was poured drop by drop into solution 2, ultrasonic irradiation was applied during 10 min, and the samples were aged for 12 h under constant agitation. The obtained powders were completely dried under vacuum at 318 K. The molar ratios used in the preparation of the composites were 1/20/0.1/30 for TEOS/water/NH_4OH/ethanol, and the nominal concentration of dye was 1×10^{-5} or 1×10^{-6} moles of dye/g of SiO_2.

2.2. Characterization. The dynamic light scattering (DLS) measurements were determined by a Zetasizer Nano instrument (Malvern), and ethanol was used as dispersant. A Quanta 3D FEG (Fei) scanning electron microscope (SEM) was used; the dry samples were deposited onto a carbon tape before analysis. The SiO_2 and SiO_2-MB samples were analyzed in an Asap 2405 (Micromeritics) automated gas sorption system to obtain the nitrogen adsorption isotherms at 77.4 K. The specific surface area was estimated with the Brunauer-Emmett-Teller (BET) model, and the pore size distribution was evaluated with the BJH model. All samples were outgassed at 373 K for 1 h prior to analysis. FTIR spectra in the region 4000–400 cm^{-1} were obtained with a Nexus 470 Spectrometer (Nicolet). The powders were mixed with KBr to form a pellet. UV-vis spectra were obtained on a Cintra 20 Spectrometer (GBC). The diffuse reflectance measurements were done using the lab sphere RSA-PE-20 accessory using $BaSO_4$ as reference. In all cases the spectra were recorded in the 400–800 nm region.

2.3. Photocatalytic Evaluation. The photooxygenation of 9, 10-dimethylanthracene (DMA) was carried out in acetonitrile (HPLC grade) using a Newport solar simulator (Model 67005) equipped with a 150 W Xe lamp with a maximum emission around 460 nm. It was used a 10 mL batch reactor for the evaluation of the SiO_2-MB composites and an 80 mL batch reactor for the evaluation of the different SiO_2-dye composites. The temperature was kept constant at 298 K, and the incident light was filtered in order to cut out light below 400 nm and eliminate any photochemical reaction of DMA. The initial concentration of DMA was 16 mg/L, and the composite loading was 1 g/L or 0.5 g/L. The reaction samples were analyzed using HPLC (GBC model 1120) equipped with a UV detector (λ = 254 nm), using a 70/30 acetonitrile/water mobile phase (1 mL/min) and a 15 cm column (Grace Prevail C18 5 μ). The samples were also analyzed using a GC-MS

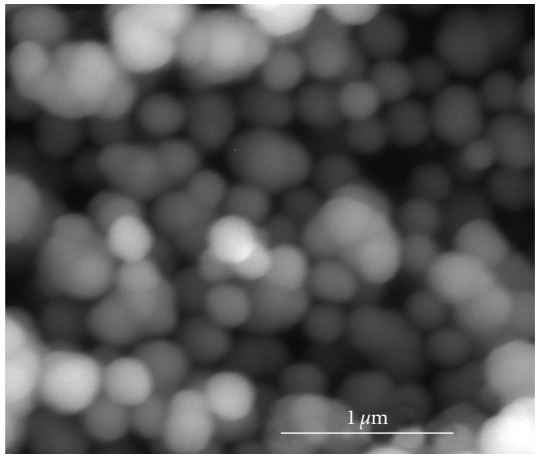

Figure 2: SEM image of SiO_2-MB composite; [MB] = 1×10^{-5} mol/g SiO_2.

(Perkin-Elmer model TurboMass) using a 30 m capillary column (Alltech EC5).

3. Results and Discussion

3.1. Characterization Results of SiO_2-MB Composites. The influence of the dye over the final particle size of the composite was determined by DLS. During the polymerization of TEOS through the formation of Si–O–Si bonds, the cationic part of MB molecule can interact with part of Si–O groups by electrostatic forces, increasing the stability of the hybrid system [17] and leading to an amount of the average size from 110 nm (as-prepared SiO_2) to 141 and 185 nm by using 1×10^{-6} and 1×10^{5} mol/g SiO_2 MB concentration, respectively. The stability of the SiO_2-MB composites was compared in a blank experiment, where a solution of MB in ethanol was mixed under stirring with the as-prepared SiO_2 particles during 12 h and then dried under vacuum and 318 K. The resulting material was rinsed with ethanol, and the MB was completely washed out, causing a total decolorization. However, the SiO_2-MB composite prepared by the modified Stöber method never exhibited this behavior. The remaining ethanol used in the SiO_2-MB composite washes was analyzed by UV-vis, and the characteristic absorption bands of MB were not observed, confirming the high stability of the composite.

A SEM image of the SiO_2-MB composite shows the morphology of the spheres in Figure 2. It can be seen spheres ranging from 100 to 200 nm in size, in some cases well dispersed but also forming particle agglomerates. The morphology of the silica spheres (not shown here) was similar than that of the composite.

Figure 3 shows the nitrogen adsorption-desorption isotherm of the SiO_2 and the SiO_2-MB composite. The shape corresponds to a type IV isotherm according to the IUPAC classification [22]. The hysteresis loop (H3/H4 types) can be attributed to the presence of slit-shaped pores and open pores where no condensation was evident. According to these results, the pore size varies between 10 and 100 nm dia-meter (see Figure 3(a)). The corresponding surface area was 91 m^2/g for SiO_2 and 23 m^2/g for the SiO_2-MB composite. Note that slight changes in the composite adsorption-desorption isotherm (Figure 3(b)) caused a dramatic decrease in specific surface area and a bimodal behavior of pore size distribution with an important amount of macropores. These results could be indicative that MB was incorporated, probably of irregular form, into the silica matrix modifying the shape and size of the pores.

Table 1: Characteristic bands of different MB species [26].

Species	Wavelength (nm)	Assignment
$(AM^+)_n$	570–590	Trimer and higher aggregates
$(AM^+)_2$	600–620	Dimer
AM^+	650–675	Monomer

FT-IR spectra of MB, SiO_2, and SiO_2-MB composite ([MB] = 1×10^{-5} mol/g SiO_2) are presented in Figure 4. The main absorption bands of MB at 1610, 1505, 1405, and 1355 cm^{-1} are assigned to the $=N^+$ cation, the heterocyclic skeleton, and to the $-CH_3$ symmetric and asymmetric bending vibrations, respectively [23, 24] (Figure 4(a)). The obtained spectrum of SiO_2 (Figure 4(b)) reproduces the general features often reported for this compound [24, 25]. It is worth noting that bands at 1200, 1100, 800, and 460 cm^{-1} are attributed to Si–O–Si vibrations and band at 960 cm^{-1} corresponds to the Si–OH vibration. The spectrum also presented a broad band located between 3750 and 3000 cm^{-1}; this can be generated by the hydration of the solid (bands located at 3350 and 1630 [24]) or by the presence of SiO–H vibrations [25]. The FT-IR spectrum of the SiO_2-MB composite was quite similar than that of SiO_2, which can be attributed to the low concentration of MB in the material, so that the main absorption bands of MB overlap with SiO_2 bands (Figure 4(c)). Note that a slight deformation of Si–O–Si bands at 1200 cm^{-1} and 3000–3750 cm^{-1} is detected in the composite which can be indicative of a bonding interaction between the organic dye and SiO_2 [17].

The visible light absorption spectra of SiO_2-MB composites and a mechanical mixture (MB + commercial SiO_2) are compared in Figure 5. In the mechanical mixture sample, a strong band appears at 670 nm and one shoulder at 610 nm (Figure 5(b)). The main band is associated to free molecules of MB (monomer, see Table 1), and the shoulder is assigned to the formation of the so-called H-aggregates (dimers) [26, 27]. In the diffuse reflectance spectrum of SiO_2-MB composite [MB] = 1×10^{-6} mol/g SiO_2 (Figure 5(a)), a wide band appears with a maximum at around 610 nm indicating that the predominant species was MB dimers. If the concentration of MB is increased to 1×10^{-5} mol/g SiO_2, the maximum of absorption is shifted to around 590 nm, which is interpreted as the formation of trimers and higher aggregates [26].

The visible light absorption spectra of the different SiO_2-dye composites prepared by the modified Stöber method and the mechanical mixture preparations are shown in Figure 6. In general, each kind of preparations presented different optical properties. For instance, the composites prepared by the modified Stöber method showed a better

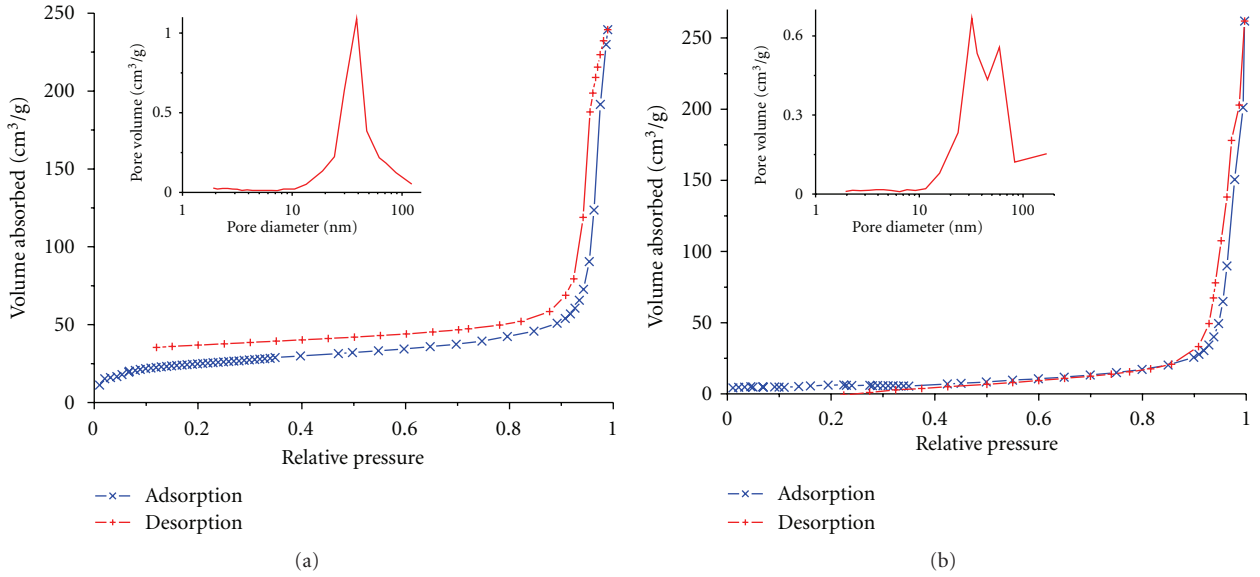

Figure 3: Nitrogen adsorption isotherms: (a) SiO_2 material as-synthesized; (b) SiO_2-MB composite; [MB] = 1×10^{-5} mol/g SiO_2.

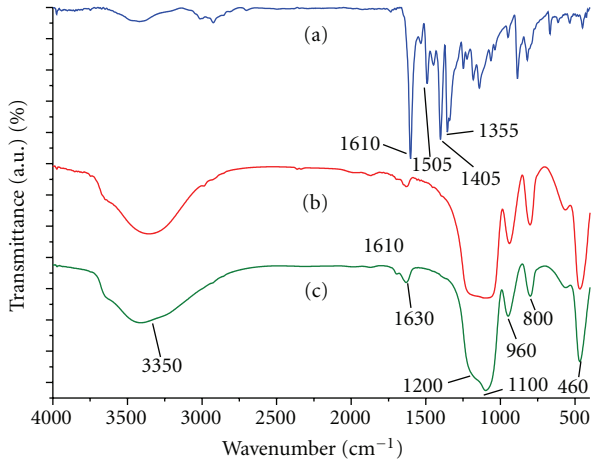

Figure 4: FT-IR spectra of (a) MB powder, (b) as-prepared SiO_2, (c) SiO_2-MB, [MB] = 1×10^{-5} mol/g SiO_2.

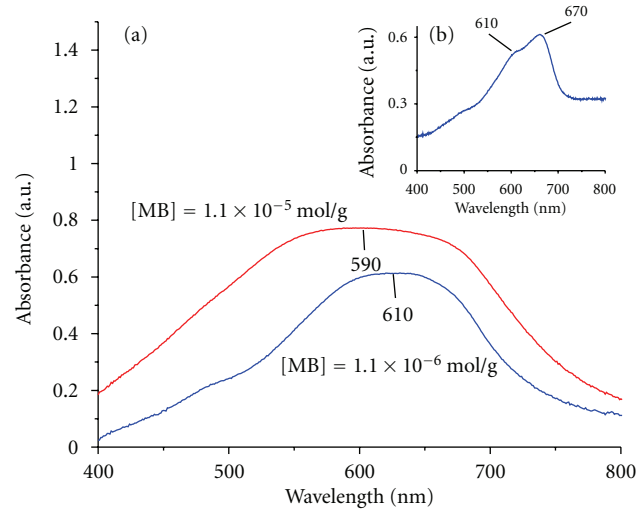

Figure 5: Visible light absorption spectra of (a) SiO_2-dye nanocomposites and (b) mechanical mixture of MB + commercial SiO_2 nanoparticles.

band definition compared with the wide and irregular profile of the mechanical mixture bands. Note that a broad absorption band with a maximum at 490 nm was observed for commercial SiO_2 + SF (Figure 6(d)); in comparison with the SiO_2-SF composite, a sharper absorption band appeared at 515 nm (Figure 6(a)). These results indicated that, in the first case, dye aggregates were the predominant species meanwhile; in the second case there were more monomeric dye species incorporated into the silica matrix [28, 29]. The SiO_2-NR composite and its mechanical mixture are shown in Figures 6(b) and 6(e). In the mechanical mixture, a broad absorption band from 400 to 650 nm, with a maximum centered at 505 nm, was previously assigned to the absorption of H-aggregates (dimers) of the dye [29]. When the dye was incorporated since the formation of the SiO_2 matrix, a solvatochromical shift in the absorption maximum to 535 nm was absorbed, and a slight shoulder at 480 nm was also observed. The absorption band associated to the free molecules of NR is located around 535 nm [29–31], and the absorption associated with the uncharged form of NR is located around 450–460 nm in methanol [30, 32]. Hence, the predominant species in the SiO_2-NR composite was the free molecules of the dye although the neutral form (pKa = 6.8 [30]) could be present, due to basic media used in the preparation of the materials, causing the observed shoulder. In the case of TB, the mechanical mixture with commercial SiO_2 (Figure 6(f)), the absorption spectrum presented an ill-defined band with a maximum centered at 585 nm, produced by the presence of TB dimers [33, 34]. When TB was

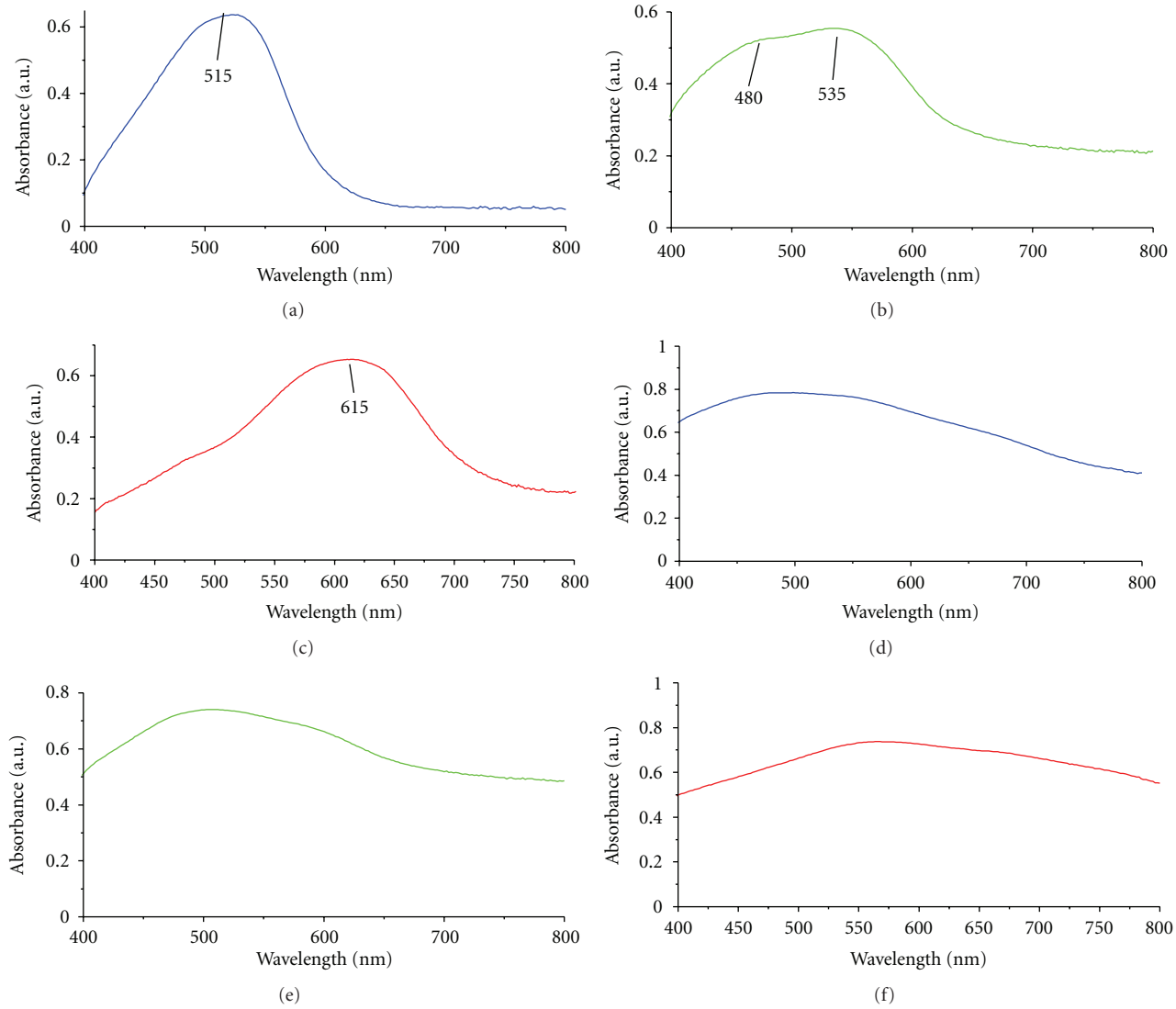

FIGURE 6: Visible light absorption spectra of SiO_2-dye composites prepared by modified Stöber method: (a) SF, (b) NR, (c) TB, and prepared by mechanical mixture with commercial SiO_2: (d) SF, (e) NR, and (f) TB.

incorporated into the SiO_2 composites (Figure 6(c)), a well-defined band appeared in the absorption spectrum centered at 615 nm and a slight shoulder also appeared at 495 nm. The absorption at 615 nm was produced by the presence of TB monomers in the composite.

3.2. Photosensitized Oxidation of DMA . In photosensitized reactions, the photosensitizer molecule absorbs the energy of a photon ($h\nu$) of ultraviolet or visible radiation to become an excited singlet state which rapidly converts into an excited triple state. The lifetime of the triplet is longer (microseconds) than that of the singlet (nanoseconds) so that energy transfer from the triplet to dissolved oxygen molecule to form singlet oxygen ($^1O_2$) is possible. The amount of singlet oxygen generated by a photosensitizer is determined by the rate of absorption of photons, the triplet quantum yield, and the efficiency of the energy transfer process [35]. After singlet oxygen is generated, it either reacts with a substrate or losses its excitation energy as heat or light emission (phosphorescence). Scheme 1 shows a reaction scheme considering the visible light irradiation of a SiO_2-dye composite in presence of oxygen, ethanol, and the main substrate DMA.

Scheme 1 (reaction scheme of the photosensitized oxidation of DMA on dye-doped silica composites).

$$\text{SiO}_2\text{-dye} + h\nu \longrightarrow \text{SiO}_2\text{-dye}^* \quad I, \tag{1}$$

$$\text{SiO}_2\text{-dye}^* + {}^3\text{O}_2 \longrightarrow \text{SiO}_2\text{-dye} + {}^1\text{O}_2 \quad k, \tag{2}$$

$$\text{DMA} + {}^1\text{O}_2 \longrightarrow \text{DMA endoperoxide} \quad k_c, \tag{3}$$

$${}^1\text{O}_2 \longrightarrow {}^3\text{O}_2 \quad k_d, \tag{4}$$

where I is the light intensity, k is a rate constant for the quenching of excited SiO_2-dye by triplet oxygen to produce

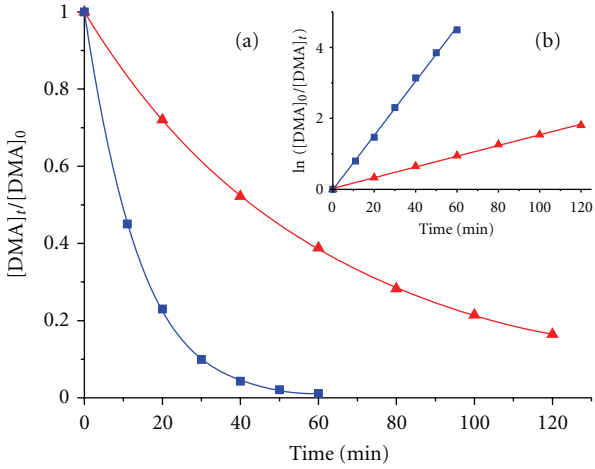

FIGURE 7: (a) Relative concentration of DMA versus time for SiO_2-MB composites (▲) [MB] = 1×10^{-6} mol/g SiO_2 (■) [MB] = 1×10^{-5} mol/g SiO_2. (b) First-order kinetics data fitting.

singlet oxygen, k_c is the rate constant of chemical quenching of singlet oxygen in presence of DMA; however, singlet oxygen also decays to the ground state by energy transfer to the solvent or with other species in solution with a rate constant k_d [36]. A rough estimation of the rate constant in (3) can be obtained by considering that an excess of singlet oxygen is produced compared with the initial concentration of DMA and then a pseudofirst-order reaction is proposed (5)–(8):

$$-\frac{d[\mathrm{DMA}]}{dt} = k_c[\mathrm{DMA}]\left[{}^1\mathrm{O}_2\right] = k'[\mathrm{DMA}], \tag{5}$$

where

$$k' = k_c\left[{}^1\mathrm{O}_2\right] = \Phi I\frac{kc}{kd}, \tag{6}$$

$$[\mathrm{DMA}]_t = [\mathrm{DMA}]_0 e^{-k't}, \tag{7}$$

$$\ln\frac{[\mathrm{DMA}]_0}{[\mathrm{DMA}]_t} = k't. \tag{8}$$

The concentration profiles of DMA, during the photooxidation in presence of SiO_2-MB, are shown in Figure 7. Note that raw data fit well to a first-order reaction at two concentrations of MB, with k' values of 0.0762 and 0.0154 min^{-1} for 1×10^{-5} and 1×10^{-6} moles of dye/g of SiO_2, respectively.

As shown in Figure 8, the conversion of DMA followed a similar behavior (first order kinetics) with the different SiO_2-dye composites. However, the rate constants had different values, and it is clearly seen that SiO_2-MB is not a good photocatalyst for this reaction. Note that the k' values had the following increasing order depending of the dye used in the photooxidation of DMA (Figure 9): SF > TB > NR > MB. These results revealed that the singlet oxygen generation depended on the type of composite used. Therefore, in the particular case of SiO_2-SF composite instead of presenting almost the same absorption properties than MB, it presented a rate constant one order of magnitude higher compared

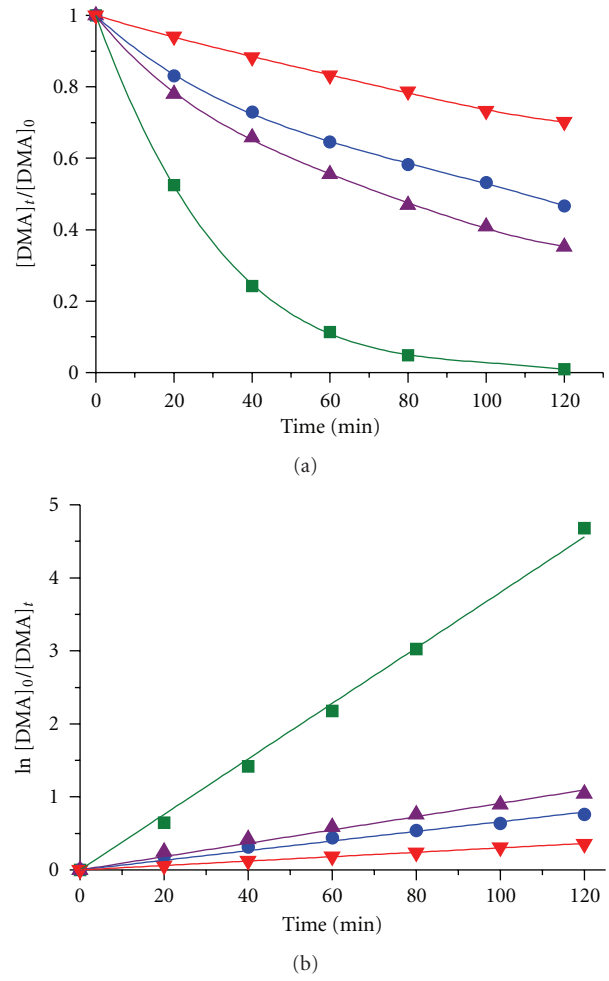

FIGURE 8: (a) Relative concentration of DMA versus time for different SiO_2-composites: (▼) MB; (•) NR; (▲) TB; (■) SF. (b) First-order kinetics data fitting.

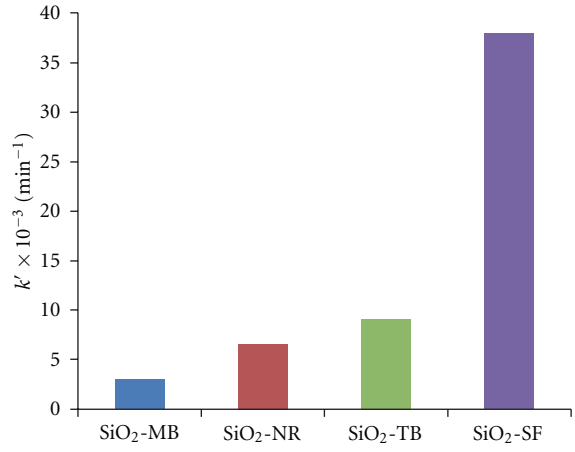

FIGURE 9: Rate constant values (k') of the photooxidation of DMA with different SiO_2-dye composites.

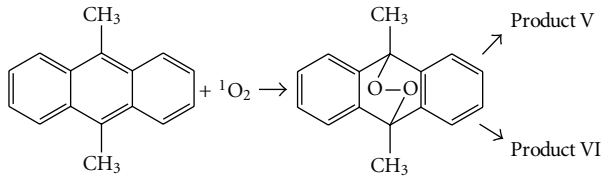

Figure 10: Reaction path scheme of DMA endoperoxide formation as well as the unidentified V and VI products detected by HPLC and GC-MS (see Supplementary Information available online at doi: 10.1155/2012/987606).

with MB which should be interpreted as SF dye was homogenously dispersed on the silica matrix, as indicated by the UV-vis spectra results (Figures 5 and 6), where the SiO_2-SF composite presented a sharper absorption band at 515 nm, mainly as a consequence of the presence of monomeric species of SF in the material. Further studies are in progress in our lab in order to know in detail the properties and behavior of the SiO_2-SF composites for fine chemical synthesis under visible light irradiation.

Finally, a reaction path scheme showing the formation of DMA endoperoxide and two unidentified byproducts (V and VI), which were found with all series of dye-doped silica particles, is presented in Figure 10. As mentioned before, the main product was the DMA endoperoxide; however, the two unidentified byproducts were detected by HPLC and GC-MS (supplementary information). As is well known, the endoperoxides are highly instable compounds so that easily decompose to other oxygenated compounds following a parallel path forming stable products as the unidentified V and VI byproducts.

4. Conclusion

In this study, a novel procedure (modified Stöber method) to obtain stable and active SiO_2-dye composites for the photosensitized oxidation of 9,10-dimethylanthracene was developed. We found important differences in the mechanical mixtures and Stöber's method preparations of our four dye-doped silica composites than can be attributed to the higher electrostatic interaction and dispersion of the dye into the silica matrix by the second procedure. According to the results, all dyes had a larger affinity to the matrix and can be easily incorporated. These findings agreed with the photocatalytic behavior, and the SiO_2-SF composite showed the most efficient delivery of $^1O_2$. Two byproducts were also detected during the photooxidation of DMA which are probably assigned to the decomposition of the endoperoxide.

Acknowledgments

This work was financially supported by the National Council of Science and Technology (Conacyt) Projects: 106891 and 153356. The authors also acknowledge the support of COFAA-IPN. E. Albiter thanks Conacyt for the scholarship support.

References

[1] C. Tanielian, C. Schweitzer, R. Seghrouchni, M. Esch, and R. Mechin, "Polyoxometalate sensitization in mechanistic studies of photochemical reactions: the decatungstate anion as a reference sensitizer for photoinduced free radical oxygenations of organic compounds," *Photochemical and Photobiological Sciences*, vol. 2, no. 3, pp. 297–305, 2003.

[2] G. Schenck, "Photosensitization," *Industrial & Engineering Chemistry*, vol. 55, no. 6, pp. 40–43, 1963.

[3] C. S. Foote, "Mechanisms of photosensitized oxidation," *Science*, vol. 162, no. 3857, pp. 963–970, 1968.

[4] C. S. Foote, "Type I and type II mechanisms of photodynamic action," in *Light-Activated Pesticides*, vol. 339, pp. 22–38, American Chemical Society, 1987.

[5] A. Greer, "Christopher Foote's discovery of the role of singlet oxygen [$^1O_2$] in photosensitized oxidation reactions," *Accounts of Chemical Research*, vol. 39, no. 11, pp. 797–804, 2006.

[6] E. L. Clennan and A. Pace, "Advances in singlet oxygen chemistry," *Tetrahedron*, vol. 61, no. 28, pp. 6665–6691, 2005.

[7] M. C. DeRosa and R. J. Crutchley, "Photosensitized singlet oxygen and its applications," *Coordination Chemistry Reviews*, vol. 233-234, pp. 351–371, 2002.

[8] J. Wahlen, D. E. De Vos, P. A. Jacobs, and P. L. Alsters, "Solid materials as sources for synthetically useful singlet oxygen," *Advanced Synthesis and Catalysis*, vol. 346, no. 2-3, pp. 152–164, 2004.

[9] S. Wang, R. Gao, F. Zhou, and M. Selke, "Nanomaterials and singlet oxygen photosensitizers: potential applications in photodynamic therapy," *Journal of Materials Chemistry*, vol. 14, no. 4, pp. 487–493, 2004.

[10] A. E. O'Connor, W. M. Gallagher, and A. T. Byrne, "Porphyrin and nonporphyrin photosensitizers in oncology: preclinical and clinical advances in photodynamic therapy," *Photochemistry and Photobiology*, vol. 85, no. 5, pp. 1053–1074, 2009.

[11] P. Couleaud, V. Morosini, C. Frochot, S. Richeter, L. Raehm, and J. O. Durand, "Silica-based nanoparticles for photodynamic therapy applications," *Nanoscale*, vol. 2, no. 7, pp. 1083–1095, 2010.

[12] T. Montagnon, M. Tofi, and G. Vassilikogiannakis, "Using singlet oxygen to synthesize polyoxygenated natural products from furans," *Accounts of Chemical Research*, vol. 41, no. 8, pp. 1001–1011, 2008.

[13] D. Gryglik, J. S. Miller, and S. Ledakowicz, "Solar energy utilization in degradation of 2-chlorophenol by immobilized photosensitizers," *Solar Energy*, vol. 77, no. 5, pp. 615–623, 2004.

[14] L. Villén, F. Manjón, D. García-Fresnadillo, and G. Orellana, "Solar water disinfection by photocatalytic singlet oxygen production in heterogeneous medium," *Applied Catalysis B*, vol. 69, no. 1-2, pp. 1–9, 2006.

[15] F. M. P. R. Van Laar, F. Holsteyns, I. F. J. Vankelecom, S. Smeets, W. Dehaen, and P. A. Jacobs, "Singlet oxygen generation using PDMS occluded dyes," *Journal of Photochemistry and Photobiology A*, vol. 144, no. 2-3, pp. 141–151, 2001.

[16] A. S. de Dios and M. E. Díaz-García, "Multifunctional nanoparticles: analytical prospects," *Analytica Chimica Acta*, vol. 666, no. 1-2, pp. 1–22, 2010.

[17] H. Yao, J. M. Hong, N. Li, S. Xu, and J. J. Zhu, "Homogenous thionine-SiO_2 nanocomposite spheres: sonochemical preparation, characterization, and application in H_2O_2 biosensor," *Journal of Nanoscience and Nanotechnology*, vol. 9, no. 4, pp. 2421–2425, 2009.

[18] A. van Blaaderen and A. Vrij, "Synthesis and characterization of colloidal dispersions of fluorescent, monodisperse silica spheres," *Langmuir*, vol. 8, no. 12, pp. 2921–2931, 1992.

[19] F. J. Arriagada and K. Osseo-Asare, "Synthesis of nanosize silica in aerosol OT reverse microemulsions," *Journal of Colloid And Interface Science*, vol. 170, no. 1, pp. 8–17, 1995.

[20] W. Stöber, A. Fink, and E. Bohn, "Controlled growth of monodisperse silica spheres in the micron size range," *Journal of Colloid And Interface Science*, vol. 26, no. 1, pp. 62–69, 1968.

[21] D. Zhang, Z. Wu, J. Xu, J. Liang, J. Li, and W. Yang, "Tuning the emission properties of $Ru(phen)_3^{2+}$ doped silica nanoparticles by changing the addition time of the dye during the stöber process," *Langmuir*, vol. 26, no. 9, pp. 6657–6662, 2010.

[22] K. S. W. Sing, D. H. Everett, R. A. W. Haul et al., "Reporting physorption data for gas/solid systems," *Pure and Applied Chemistry*, vol. 57, no. 4, p. 16, 1985.

[23] O. V. Ovchinnikov, S. V. Chernykh, M. S. Smirnov et al., "Analysis of interaction between the organic dye methylene blue and the surface of AgCl(I) microcrystals," *Journal of Applied Spectroscopy*, vol. 74, no. 6, pp. 809–816, 2007.

[24] K. Nakanishi and P. H. Solomon, *Infrared Absorption Spectroscopy*, Holden-Day, San Francisco, Calif, USA, 1977.

[25] G. D. Chukin and V. I. Malevich, "Infrared spectra of silica," *Journal of Applied Spectroscopy*, vol. 26, no. 2, pp. 223–229, 1977.

[26] J. J. Beaudoin, B. Patarachao, L. Raki, and R. Alizadeh, "Adsorption of methylene blue as a descriptor of C-S-H nanostructure," *Cement and Concrete Composites*, vol. 33, no. 2, pp. 246–250, 2011.

[27] D. Madhavan and K. Pitchumani, "Reactions in clay media: photooxidation of sulfides by clay-bound methylene blue," *Tetrahedron*, vol. 57, no. 39, pp. 8391–8394, 2001.

[28] M. L. Gómez, C. M. Previtali, and H. A. Montejano, "Photophysical properties of safranine O in protic solvents," *Spectrochimica Acta A*, vol. 60, no. 11, pp. 2433–2439, 2004.

[29] L. Antonov, G. Gergov, V. Petrov, M. Kubista, and J. Nygren, "UV-Vis spectroscopic and chemometric study on the aggregation of ionic dyes in water," *Talanta*, vol. 49, no. 1, pp. 99–106, 1999.

[30] M. K. Singh, H. Pal, A. C. Bhasikuttan, and A. V. Sapre, "Dual solvatochromism of neutral red," *Photochemistry and Photobiology*, vol. 68, no. 1, pp. 32–38, 1998.

[31] F. Gessner, C. C. Schmitt, and M. G. Neumann, "Time-dependent spectrophotometric study of the interaction of basic dyes with clays. 1. Methylene blue and neutral red on montmorrillonite and hectorite," *Langmuir*, vol. 10, no. 10, pp. 3749–3753, 1994.

[32] J. Mohanty, A. C. Bhasikuttan, W. M. Nail, and H. Pal, "Host-guest complexation of neutral red with macrocyclic host molecules: contrasting pK_a shifts and binding affinities for cucurbit[7]uril and β-cyclodextrin," *Journal of Physical Chemistry B*, vol. 110, no. 10, pp. 5132–5138, 2006.

[33] M. Ilanchelian, C. Retna Raj, and R. Ramaraj, "Spectral studies on the Cyclodextrin inclusion complexes of toluidine blue O and Meldola's blue in aqueous solution," *Journal of Inclusion Phenomena*, vol. 36, no. 1, pp. 9–20, 2000.

[34] J. Jebaramya, M. Ilanchelian, and S. Prabahar, "Spectral studies of toluidine blue o in the presence of sodium dodecyl sulfate," *Digest Journal of Nanomaterials and Biostructures*, vol. 4, no. 4, pp. 789–797, 2009.

[35] C. S. Foote, "Photosensitized oxygenations and the role of singlet oxygen," *Accounts of Chemical Research*, vol. 1, no. 4, pp. 104–110, 1968.

[36] W. Tang, H. Xu, R. Kopelman, and M. A. Philbert, "Photodynamic characterization and in vitro application of methylene blue-containing nanoparticle platforms," *Photochemistry and Photobiology*, vol. 81, no. 2, pp. 242–249, 2005.